Use of Visible and Near Infrared Spectral Reflectance in Determining Damage from *Diaprepes Abbreviatus*

M. Borengasser, K.D. Hutchenson
ENSCO, Inc.
Melbourne, FL USA

C.H. Blazquez
Sensor Systems Laboratory
Cocoa Beach, FL USA

R.C. Adair
The Kerr Center
for Sustainable Agriculture
Vero Beach Research Station
Vero Beach, FL USA

ABSTRACT

A relatively new technique to detect damage in Ruby Red grapefruit trees from *Diaprepes abbreviatus*, a non-native root weevil, was used. The study area was the Kerr Center for Sustainable Agriculture in east central Florida. Trees infested with *D. abbreviatus* were divided into four categories based on reduction of canopy density. A relationship was observed between the stage of decline of the tree and the spectral signature. As the trees progressed toward more advanced stages of decline, an absorption feature in the near-IR became more pronounced. The first derivatives of the near-IR absorption feature and the spectral curve in the visible spectrum also correlated well with the stage of decline. As the condition of the tree deteriorated due to *D. abbreviatus*, the first derivative increased. The results suggest that *D. abbreviatus* can cause a change in the spectral reflectance, and the amount of change is dependent on the degree of damage to the tree.

INTRODUCTION

A technique that uses the visible and near-IR spectral reflectance signature was used to detect damage in citrus trees from *D. abbreviatus*, a non-native root weevil. The result of this effort suggests that *D. abbreviatus* could change the spectral reflectance signature; the degree of change was dependent on the level of damage to the tree.

D. abbreviatus was first detected in Florida citrus near Apopka in 1964 (Woodruff, 1964). No known methods will eradicate the weevil, although some controls will kill the adult weevils. Economic damage is done by the larvae, which can eventually kill the tree. The *D. abbreviatus* root weevil has slowly spread to nearly every citrus-producing county in Florida (Figure 1).

Although this effort concentrated on damage to Ruby Red grapefruit trees from *D. abbreviatus*, other studies have shown that different organisms attack different parts of the tree system (Gausman *et al.*, 1969). For example, *D. abbreviatus* larva attack the root system of the citrus tree, making the tree susceptible to *Phytophthora sp.*, a secondary pathogen, and limiting the ability of the tree to support a large canopy. One of our future goals is to construct a library of spectral signatures that relate different organisms and diseases to the stage of decline of a citrus tree. Advances in technology permit these types of measurements to be made quickly and cheaply, assisting growers and plant scientists.

DATA ACQUISITION

The equipment previously described by Blazquez *et al.* (1996) was used for this study. A SD-1000 miniature (0.22 mm) fiber optic spectrometer (Ocean Optics, Dunedin, FL) was used with a fiber optic reflectance probe, providing a potential spectral range from 361 to 900 nm. The SD-1000 was connected to a laptop computer (166 MHz Pentium) via a PCMCIA card that provided 5 V of power. Data collection software was provided by Ocean Optics (Blazquez *et al.*, 1996). All measurements were taken in November and December 1997 between 1000 and 1500 Eastern Daylight Time under conditions of bright sun. Individual files were stored in ASCII format for later analysis using MatLab (MathWorks) and Excel (MicroSoft).

STUDY AREA

Kerr Center Vero Beach Research Station (VBRS)

The VBRS consists of 35 acres of citrus groves located in the heart of the Indian River Citrus District northwest of Vero Beach, Florida (Figure 1). The VBRS is the subtropical research station for the Oklahoma-based Kerr Center, specializing in sustainable agricultural practices that are both economically and environmentally efficient.

For a number of years, a major goal of agricultural research has been to develop methods to control and eradicate *D. abbreviatus*. Since 1964, this non-native root weevil has spread to 18 counties and was reported by the Florida Department of Plant Industry to infest 22,000 acres of commercial citrus in 1994 (Adair, 1994). Early attempts to eradicate *D. abbreviatus* with chemical insecticides were unsuccessful (Bullock *et al.*, 1988). Currently there are no chemical pesticides that will eradicate the *D. abbreviatus* root weevil, although some controls will kill the adults. Both the adult and larvae attack citrus tress, although the economic damage comes from the larvae because they eventually kill the tree. The *D. abbreviatus* root weevil has slowly spread to nearly every citrus producing county in Florida.

The Ruby Red grapefruit trees at the VBRS are on *Swingle citremelo* rootstock. These trees have a population of *D. abbreviatus* that ranges from almost no insects or a light infestation to an abundant, visible infestation. Surrounding groves show distinctive stress patterns associated with the *D. abbreviatus* root weevil. The VBRS provided a unique environment to test the current method of detecting the presence of *D. abbreviatus* by specific patterns of visible and near-IR reflectance associated with the degradation of the tree.

In addition to the VBRS, a second site was visited during the investigation. This site was a small grove (approximately 1 to 2 acres), owned by Ms. Cloe Parks, in central Brevard County (Figure 1). No evidence of *D. abbreviatus* has been found in Brevard County. This is an all-natural grove; fertilization and pest control techniques use all natural compounds.

Life Cycle of D. Abbreviatus

The life cycle of *D. abbreviatus* may vary, lasting generally between one to two years. There are two periods when adult weevils emerge from the soil to attack a tree, in spring (May to June) and in fall (August to September). Eggs are laid between two leaves during both periods; a single female may lay as many as 5,000 eggs during her three to four month life span. After hatching within seven to ten days, the larvae drop to the ground and burrow into the soil to feed on the roots and other organic material, attacking larger roots as they mature. After feeding, they pupate in the soil, emerging as adults to renew the life cycle (Figure 2).

METHODOLOGY

The categories of decline of infested Ruby Red grapefruit trees were established as a qualitative measure based on reduction of canopy density. Category 0 represented a Ruby Red grapefruit tree with no infestation and a full, healthy canopy. Category 1 represented a Ruby Red grapefruit tree infected with a visible population of *D. abbreviatus* and minor leaf damage. Category 2 represented a Ruby Red grapefruit tree in a clearly stressed state with a weakened, moderately thin canopy. Category 3 represented a Ruby Red grapefruit tree canopy that was very thin and typically had no fruit. The Category 3 tree was stressed not only with *D. abbreviatus*, but numerous other diseases that occurred because of the weakened state. In this condition, the Ruby Red grapefruit tree was of no economic value and was typically abandoned or destroyed by the grower.

ANALYSIS

The field sampling methodology used in this research project produced a dataset of spectral curves of Ruby Red grapefruit trees in various stages of decline from *D. abbreviatus*. The spectral curves of trees from each category were compared to establish a degree of overall similarity. This comparison included spectral curves of leaves from the same trees, spectral curves from nearby trees, and spectral curves from trees in neighboring groves. The spectral curves for each category generally only differed by a constant reflectance value, and their specific absorption or reflectance features were very similar. This similarity in spectral reflectance for a given category justified the averaging of the spectral curves. For each category, all the spectral curves were averaged to produce a representative for that stage of decline. Figure 3 shows the representative curves for each category. A comparison of the curves before and after averaging showed that averaging retained specific spectral features while capturing the overall character of the spectral signature for a given category.

The SD-1000 spectrometer measures spectral reflectance from 361 to 900 nm in 1100 channels. Based on the spectral reflectance and absorption pattern for citrus trees in this wavelength region, the spectral curves were divided into two parts. Each curve from Figure 3 was divided into a visible component from 500 to 700 nm and a near-IR

component from 680 to 830 nm. Each of the two spectral regions was characterized by curves that were less complex and easier to model than the entire 361-900 nm range.

A major goal of the analysis process was to develop an expression or polynomial that would describe the spectral curves. This process was facilitated both by averaging the spectral curves for each category and extracting less complex yet important spectral regions. Using a curve-fitting algorithm, polynomials that approximate each curve were obtained.

The first derivative of a spectral curve is the rate of change of reflectivity with respect to wavelength. The first derivative was calculated from the polynomial for each spectral curve in the four categories. The derivative calculations were used to enhance differences in the spectral signature of Ruby Red grapefruit trees in varying stages of decline.

DISCUSSION

Comparison of Spectral Signatures – Near-IR

As the Ruby Red grapefruit trees experienced increasingly advanced stages of decline, the red edge of the near-IR reflectance showed the typical shift toward shorter wavelengths (Figure 4). The spectral region from 700 to 850 nm also correlated with the stage of decline. The trees that were unaffected *by D. abbreviatus* (Category 0) showed a slight, uniform increase in reflectance from about 750 to 785 nm. From 785 to 825 nm, reflectance decreased at a constant rate of about 15%. The spectral reflectance is approximately constant from 825 to 850 nm (Figure 4).

For Ruby Red grapefruit trees with only a slight amount of damage from *D. abbreviatus* (Category 1), the change in spectral reflectance from 700 to 850 nm was noticeably different (Figure 4). From 750 to 785 nm, reflectance decreased slightly instead of increasing. Considerable difference was apparent in the slight absorption feature near 765 nm. This absorption feature had a magnitude of about 8% reflectance. In the 785-825 nm region, reflectance decreased about 10%, and from 825 to 850 nm, reflectance decreased the same as the trees in Category 0 (Figure 4). Trees in Category 1 did not show a significant shift of the red edge to shorter wavelengths.

One group of spectral signatures came from a tree that appeared to be between Category 0 and Category 1 (Figure 4). This spectral curve showed no shift of the red edge, but the absorption feature seen near 765 nm was present with about 2% reduction in reflectance. The rest of the curve, from 785 to 850 nm, appeared to be an average of the spectral curves from Category 0 and Category 1.

The spectral curve for trees in Category 2 is shown in Figure 4. A noticeable difference from the two previous categories is the shift of the red edge of the near-IR reflectance toward shorter wavelengths. The shift is at least 10 nm in the region of 700-725 nm. The absorption feature observed at about 765 nm shifted to 770 nm, which represents approximately an 8% reduction in reflectance, as with Category 1. From 775 to 825 nm,

the reflectance decreased rapidly, being reduced by approximately 85% (Figure 4). Beyond 825 nm, the reflectance falls to zero within about 15 nm (Figure 4).

The spectral signature for Ruby Red grapefruit trees in an advanced stage of decline (Category 3) is also shown in Figure 4. The red edge of the near-IR reflectance shifted to shorter wavelengths. The shift was about 10 nm closer to the visible than for trees in Category 2. The rest of the spectral curve, from 750 to 825 nm, is similar to the spectral curve for trees in Category 2. An absorption feature was still present at approximately 770 nm and represented about 6% reduction in reflectance. From 775 to 825 nm the reflectance decreased by about 85%, similar to the spectral curves for Category 2.

Comparison of Spectral Signatures – Visible

The spectral signature for Ruby Red grapefruit trees in the visible portion of the spectrum was examined from 500 to 700 nm. As evident in Figure 5, the spectral signatures were consistent with those of stressed vegetation in general. As the condition of a tree declined, the reflectance increased, especially in the range of 525-650 nm. Table 1 shows the characteristics of the reflectance for each stage of decline for the wavelength peak at approximately 560 nm, and the spectral region from 500 to 600nm and 600 to 700 nm.

Table 1. Characteristic decline for each stage relative to 560 nm.

Category	Magnitude (560 nm)
0	7%
1	11%
2	13%
3	24%

Analysis of Spectral Curves using the First Derivative – Near-IR

The absorption feature at approximately 765 nm appeared to be correlative with the stage of decline of the Ruby Red grapefruit trees. The first derivative was calculated for the same near-IR spectral range of 680-820 nm to enhance this absorption feature and the red edge (Figure 6).

At approximately 765 nm, the first derivative, or rate of change in reflectance with respect to wavelength, appeared to correlate well with the stage of decline of the Ruby Red grapefruit trees. For Category 0, the first derivative was approximately -2.5, and for Categories 2 and 3 the first derivative was -15 and -21 respectively. Category 1 did not fit into the pattern as clearly because the first derivative was approximately -20. The reason for this difference is unclear but could be related to the different atmospheric

conditions for Category 1 measurements from the measurements for Categories 0, 2, and 3.

The red edge of the near-IR reflectance also correlated with the stage of decline in the spectral range of 685-705 nm and a first derivative between 0 and 20. As the tree progressed through increasing stages of decline, the first derivative of the spectral curve shifted toward shorter wavelengths. This relationship was not observed with the unenhanced spectral signatures.

Analysis of Spectral Curves using the First Derivative – Visible

Figure 7 shows the first derivative of the spectral curves from 500 to 680 nm. The spectral region from 500 to 560 nm correlated well with the stages of decline of the Ruby Red grapefruit trees. As the tree progressed through increasing stages of decline, the first derivative of the spectral curve increased. For each stage of decline, the maximum value of the first derivative was centered at approximately 528 nm but appeared to shift slightly toward shorter wavelengths as the stage of decline increased. Table 2 shows the relationship between the stage of decline and the associated first derivative.

Table 2. Characteristic first derivative decline for each stage.

Category	First Derivative	Maximum Wavelength
0	9%	529
1	15%	528
2	18%	528
3	30%	526

CONCLUSIONS

As the sampled Ruby Red grapefruit trees progressed from a healthy state to an advanced stage of decline from *D. abbreviatus*, the spectral signature showed associated changes. These changes were observed within the 500-600 nm and 680-830 nm portions of the spectrum, the two wavelength regions chosen for this analysis. From a visual comparison of the spectral curves, a relationship was observed between the stage of decline (Category 0-3) and the spectral signature in both of the two spectral regions. In the near-IR, an absorption feature about 10 nm wide and centered at 765 nm correlated with the stage of decline. As the Ruby Red grapefruit trees progressed toward more advanced stages of decline, the absorption feature at 765 nm became more pronounced (Figure 4). In the visible part of the spectrum, changes in the spectral curve were observed that also correlated with the stage of decline, although these spectral changes can usually be seen

in stressed vegetation in general. Specifically, as the stage of decline became more advanced, the spectral reflectance increased in the range of 525 to 650 nm (Figure 5).

The first derivative of the spectral curve made the relationship between the spectral reflectance and the stage of decline more apparent. In both of the spectral regions analyzed in this study, the first derivative of the spectral curve showed a direct correlation to the stage of decline. In the near-IR, the first derivative of the absorption feature at 765 nm increased as the Ruby Red grapefruit trees progressed through greater stages of decline (Figure 6). The first derivative ranged from about -2.5 for healthy trees (Category 0) to about -21.0 for trees in the most advanced stage of decline (Category 3). In the near-IR spectral range of 680-820 nm, the first derivative of the absorption feature at 765 nm appeared to be a reliable indicator of the stage of decline of a Ruby Red grapefruit tree from *D. abbreviatus*.

In the visible portion of the spectrum, the first derivative of the spectral curve in the region of 500-560 nm also correlated well with the stage of decline. As the condition of the tree deteriorated due to *D. abbreviatus*, the first derivative increased (Figure 7). For a healthy Ruby Red grapefruit tree, the first derivative was about 9.0 and increased to about 30.0 for trees in the most advanced stage of decline. The first derivative of the spectral curve in the range of 500-560 nm also appeared to be a reliable indicator of the condition of the Ruby Red grapefruit tree in areas where *D. abbreviatus* was present.

The resolution of the SD-1000 spectrometer is much greater than necessary to measure the spectral features from 500 to 560 nm and at approximately 765 nm. In addition, the spectral curves of leaves from the same tree, and leaves from other trees with an equivalent stage of decline were very similar. These two observations suggest that the type of measurements performed in this study could be acquired remotely, especially when considering the large areal extent of Ruby Red grapefruit trees. An airborne imaging spectrometer with spectral resolution of at least 2-3 nm and spatial resolution less than 1 m has great potential for facilitating this type of analysis over a large area. When spaceborne remote sensing systems are available that meet these spectral and spatial resolution requirements, routinely assessing the magnitude and extent of damage to Ruby Red grapefruit trees from *D. abbreviatus* could be practical and affordable.

REFERENCES

Adair, R.C. (1994). A four-year field trial of entomopathogenic nematodes for control of *Diaprepes abbreviatus* in a flatwoods citrus grove, *Proc. Fla. State Hort. Soc.*, **107**, 63-68.

Blazquez, C.H., H.N. Nigg, L.E. Hedley, L.E. Ramos, and S.E. Simpson (1996). Field assessment of a fiber optic spectral reflectance system, *Hort Technology*, **6**, No. 1, 73-76.

Bullock, R.C., C.W. McCoy, and J. Fojtik (1988). Foliar sprays to control adults of the citrus root weevil complex in Florida, *Proc. Fla. State Hort. Soc.*, **101**, 1-5.

Diaprepes Task Force (1994). Diaprepes Root Weevil, Florida Department of Agriculture.

Florida Dept. of Agriculture and Consumer Services (1997). Detections of *Diaprepes abbreviatus* in Florida for survey period 3/18/97 – 7/24/97, Division of Plant Industry, Bureau of Pest Eradication and Control.

Gausman, H.W., W.A. Allen, R. Cardenas, and M. Schupp (1969). The influence of cyclocel treatment of cotton plants and foot rot disease of grapefruit trees on leaf spectra in relation to aerial photographs with infrared color film, *Proc. 2nd Wksp. Aerial color Photo, Plant Sci., Amer. Soc. Photogramm.*, **2**, 2-10.

Woodruff, R.E. (1964). A Puerto Rican weevil new to the United States (Coleoptera: Curculionidae), *Fla. Dept. Agr., Plant Ind.*, Entomol. Cir. No. 77, 1-4

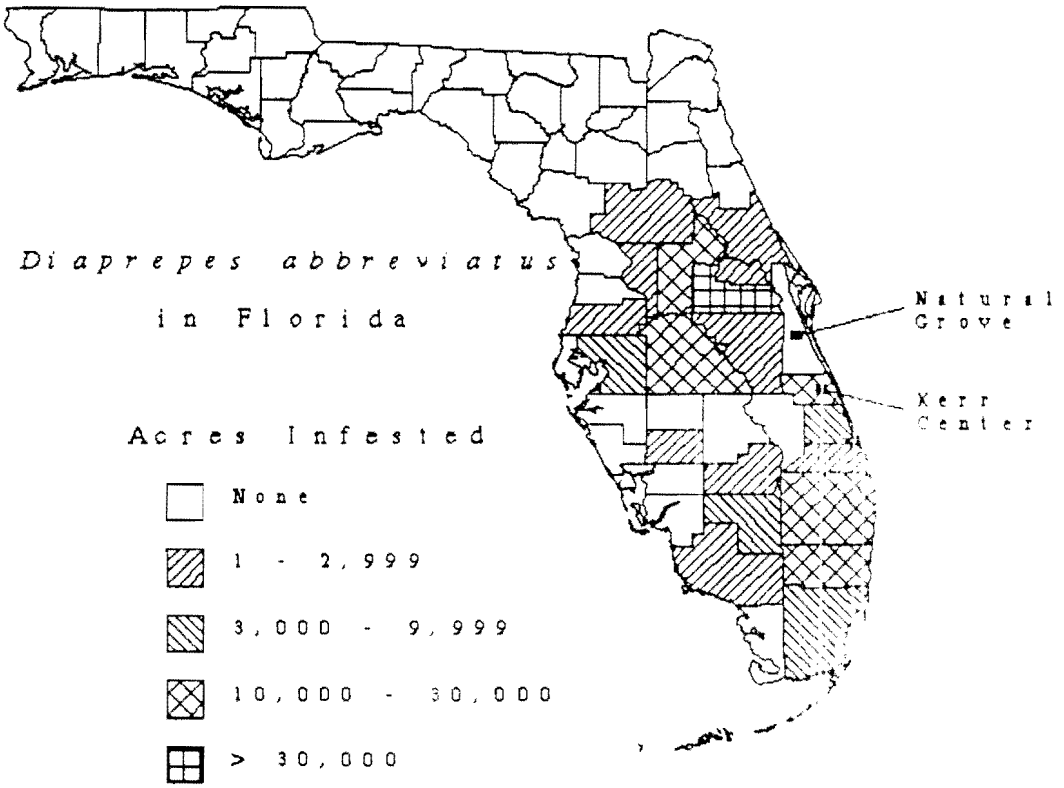

Figure 1. Location of the two study areas and distribution of *D. abbreviatus* in Florida (modified from FL Dept. Agriculture and Consumer Service, 1997)

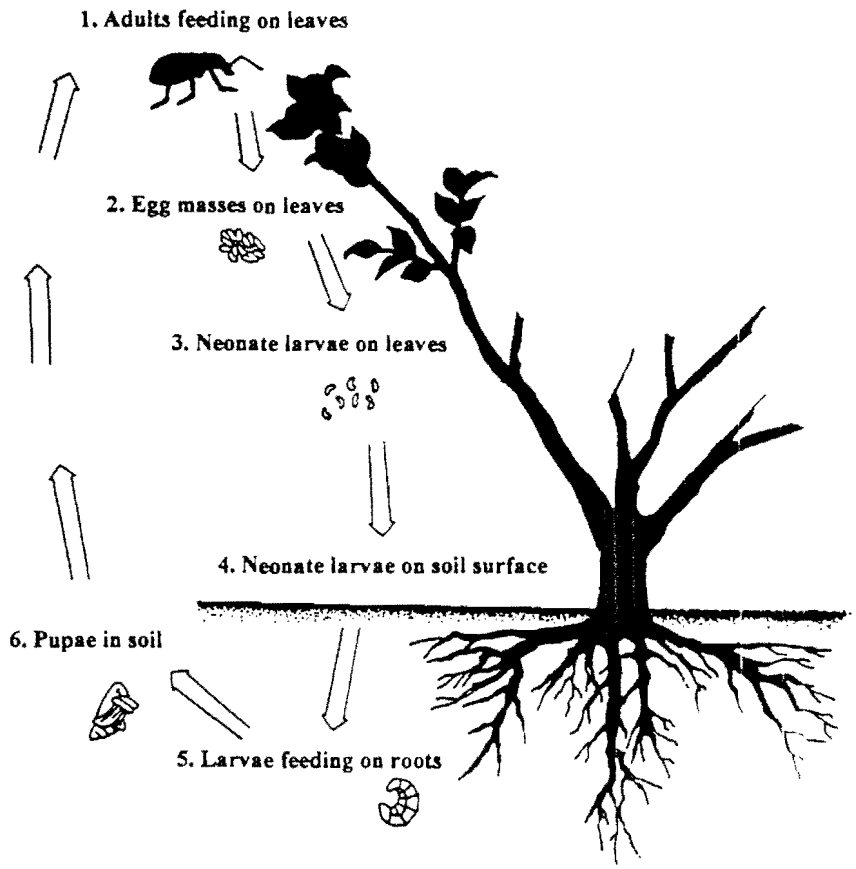

Figure 2. Life cycle of *D. abbreviatus* (modified from Diaprepes Task Force, 1994).

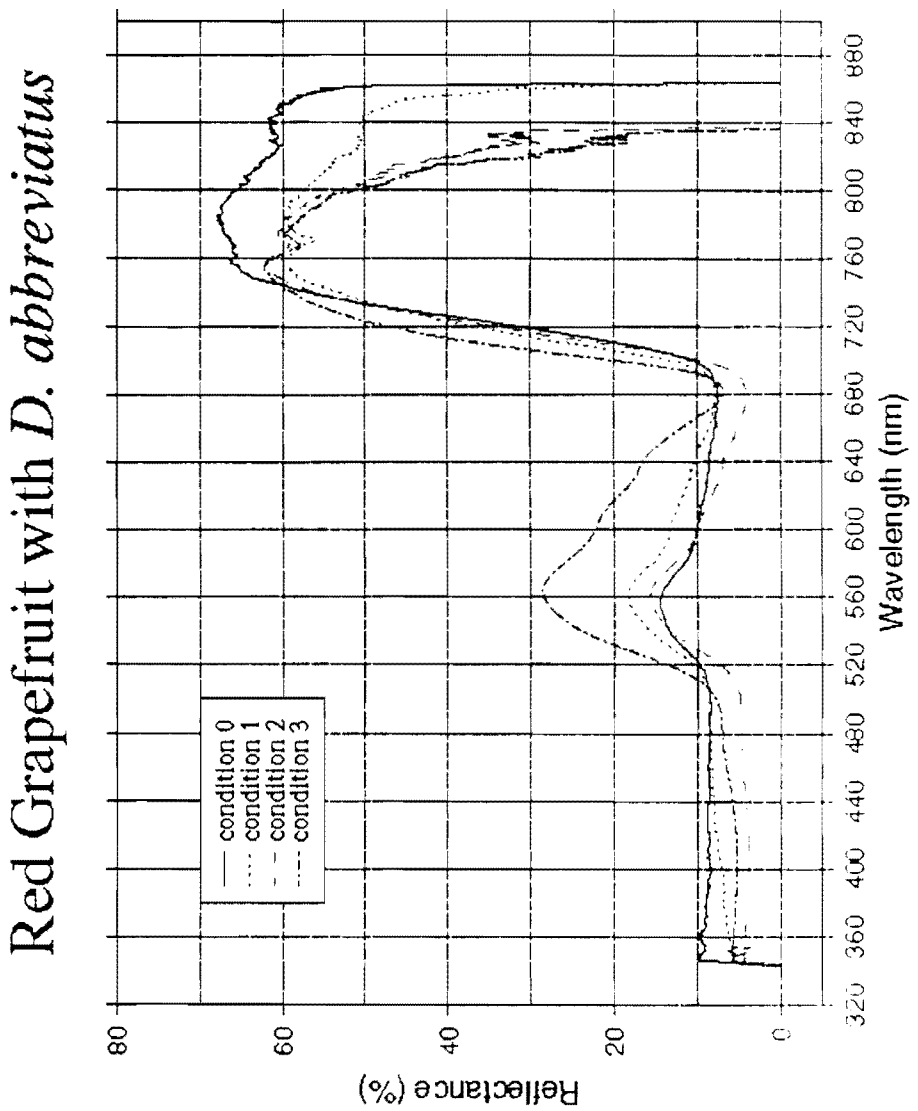

Figure 3. Spectral curves organized by category.

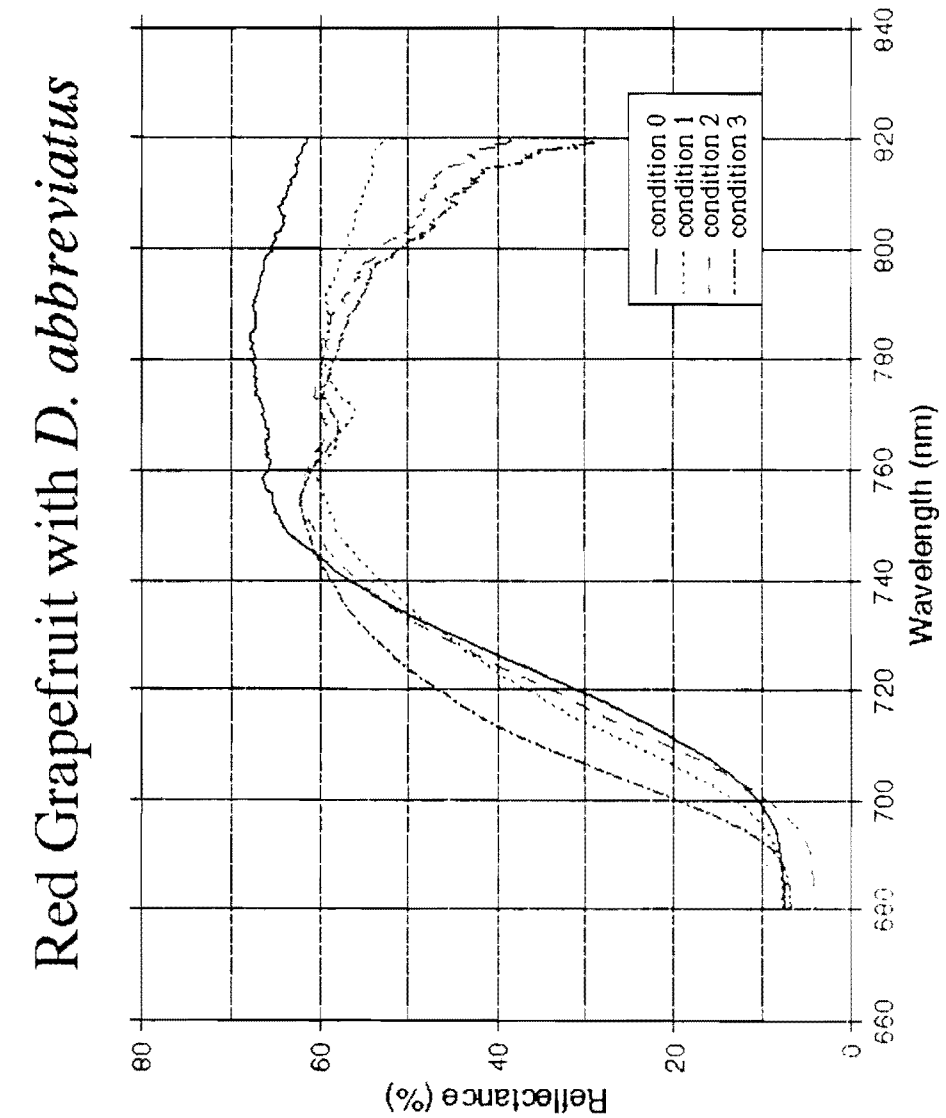

Figure 4. Polynomial curves for each category in the near-IR region between 680 and 830 nm.

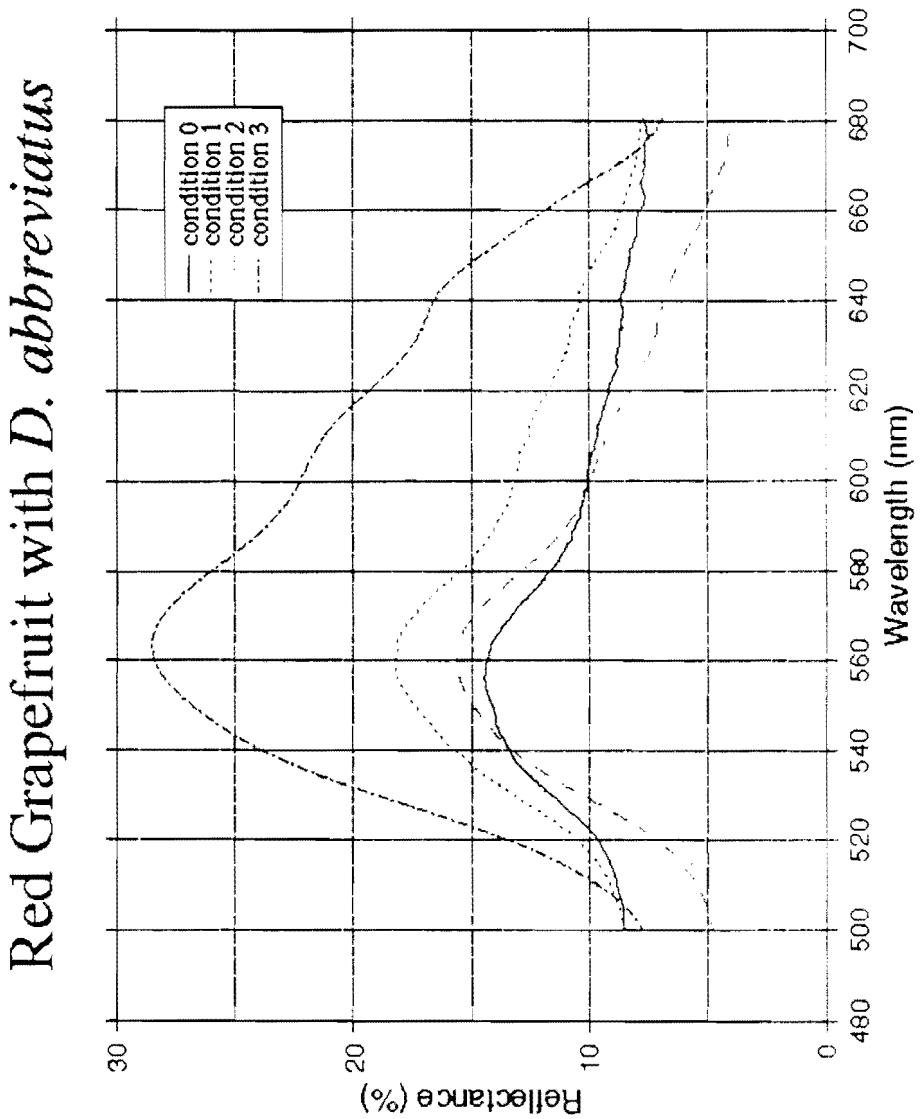

Figure 5. Polynomial curves by category in the visible region between 500 and 600 nm.

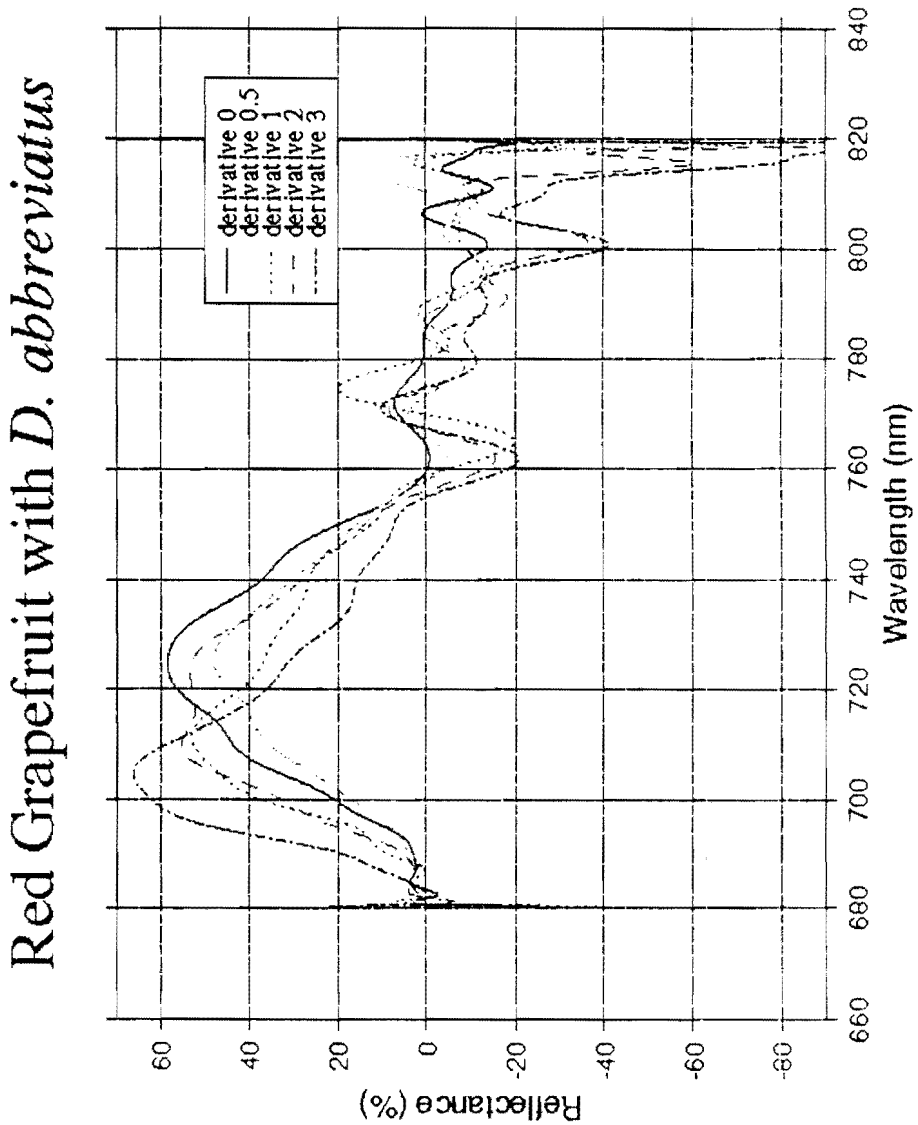

Figure 6. First derivative of the polynomial curves by category in the near-IR region between 680 and 830 nm.

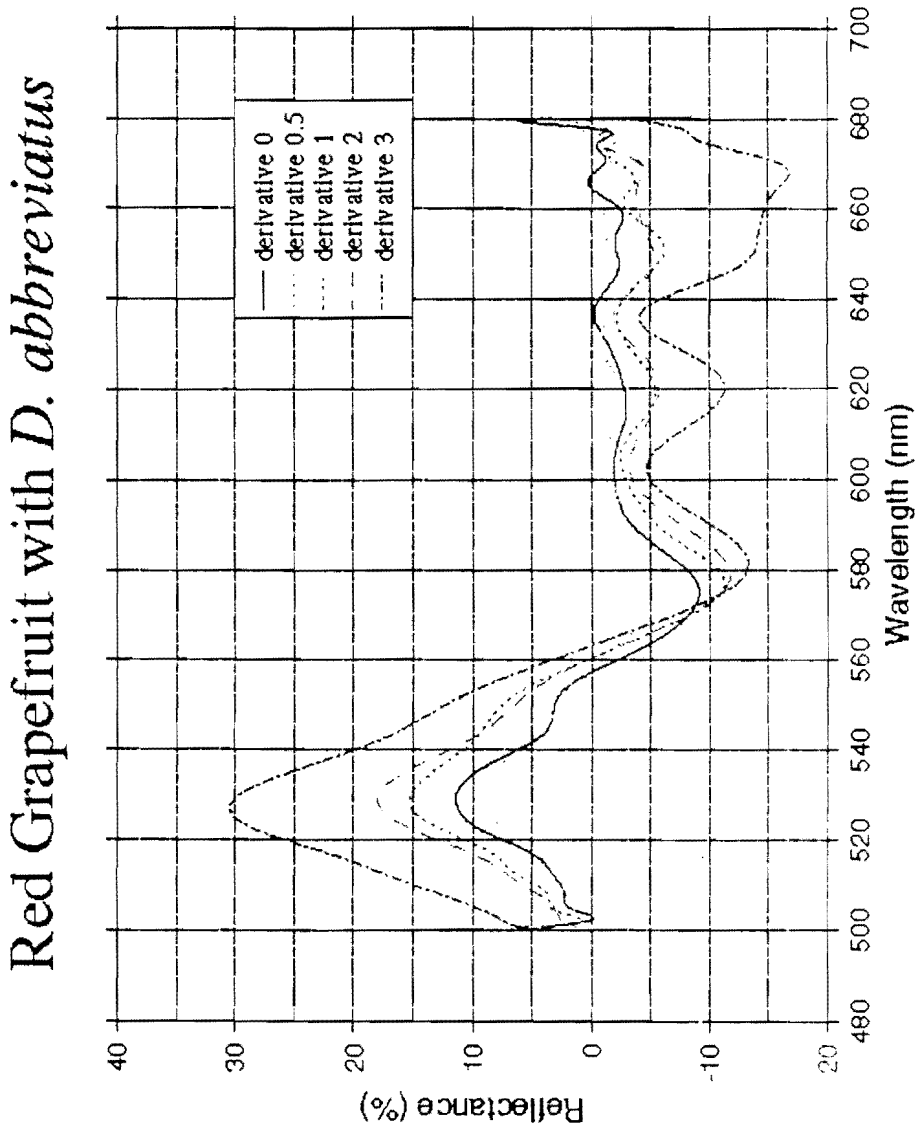

Figure 7. First derivative of the polynomial curves by category in the visible region between 500 and 600 nm.